Analytical expression for the dislocation contrast factor of the ⟨001⟩{100} cubic slip-system: Application to Cu_2O

Jorge Martinez-Garcia, Matteo Leoni, and Paolo Scardi*
Department of Materials Engineering and Industrial Technologies, University of Trento, via Mesiano 77, 38050 Trento, Italy
(Received 29 May 2007; revised manuscript received 30 August 2007; published 28 November 2007)

An analytical solution was obtained for the average contrast factor $\bar{C}_{hkl}$ of dislocations with ⟨001⟩{100} slip-system in anisotropic cubic crystals. The expression provides the dislocation contrast factor as an explicit function of the Miller indices (*hkl*), the elastic anisotropy factor A_z, and the Poisson ratio ν, thus avoiding lengthy numerical calculations or approximate parametrizations. The expression was incorporated in the whole powder pattern modelling algorithm and used to study dislocations in ball milled nanocrystalline Cu_2O.

DOI: 10.1103/PhysRevB.76.174117 PACS number(s): 61.72.Hh, 61.10.Nz, 61.82.Rx, 61.72.Lk

INTRODUCTION

Diffraction techniques are frequently used to study microstructure, lattice defects, and plastic deformation in materials, as they are very sensitive to the local atomic arrangement. In particular, the long range strain field of dislocations distorts the crystal lattice in such a way that dislocations can be directly observed in transmission electron microscopy[1] as well as in x-ray diffraction (XRD) patterns, through a characteristic line broadening effect[2–5].

The study of dislocations by XRD line profile analysis (LPA) is a relatively old issue, dating back to the pioneering works of Wilson, Krivoglaz, and Wilkens in the 1950s and 1960s. Relations between peak profile parameters describing the line broadening (e.g., integral breath, Fourier coefficients, and full width at half maximum of the line profile) and dislocation parameters (e.g., Burgers vector, edge-screw character, density, and effective outer cut-off radius) have been established within the frame of the kinematical diffraction theory.[2–5] The inclusion of these results into state of the art LPA methods has led to whole powder pattern modeling (WPPM), a very powerful technique for the study of crystalline domain size and/or shape, dislocations and other lattice defects in powder or in bulk polycrystalline materials[6–9].

A fundamental step in determining dislocation parameters from the broadened XRD profiles is the evaluation of the so-called average dislocation contrast factor $\bar{C}_{hkl}$ appearing in the theoretical expression of the XRD peak profile. As the contrast factor depends both on the elastic properties of the material (single crystal elastic constants) and on the dislocation type and orientation with respect to the diffraction vector $\mathbf{d}^*$, it carries most of the information on the line broadening anisotropy[3,10].

The calculation of $\bar{C}_{hkl}$ follows the early works of Krivoglaz and Ryaboshapka,[3] Krivoglaz,[4,11] and Wilkens.[5,12] A general formalism for its evaluation was presented by Klimanek and Kužel (KK),[13–15] who gave a comprehensive account of the dislocation contrast factor in hexagonal crystals, also providing an analytical expression for $\bar{C}_{hkl}$ in the limit of isotropic elasticity. Later on, Ungár and co-workers[16–18] proposed a parametrization of $\bar{C}_{hkl}$ for some slip-systems in cubic and hexagonal materials and published the corresponding parameters for selected materials. Recently, dislocation contrast factor calculation and use was generalized to any slip-system of any crystal symmetry, and examples for tetragonal and monoclinic materials were provided.[19]

The evaluation of $\bar{C}_{hkl}$ in real materials involves the calculation of the displacement field of a dislocation in an anisotropic medium. The traditional procedure passes through the evaluation of the roots of a sextic equation which, in the general case, cannot be obtained analytically.[20] As a consequence, contrast factor calculations have always been carried out numerically. Even if numerical procedures may be perfectly adequate to give precise values,[16–18,21] a clear correlation between slip-system, elastic properties of the material, and $\bar{C}_{hkl}$ cannot be obtained, and one has to limit to empirical relations.[15–17]

In cases of favorable orientation of the dislocation slip-system with respect to the symmetry axes of the unit cell, the sextic equation simplifies and analytical roots can be obtained.[22] This approach is here applied to the ⟨001⟩{100} slip-system in cubic materials, relevant, e.g., to Cu_2O,[23] a material of considerable technological interest with some peculiar elastic properties.[24] In particular, $\bar{C}_{hkl}$ is obtained in a closed analytical form, as a function of *hkl*, Zener ratio A_z (also known as anisotropy factor, see the Appendix), and the Poisson ratio ν. Besides matching the numerical values for Cu_2O,[21,24] the analytical expressions can easily be used for all cuprous oxide isomorphs, just by using the appropriate elastic constants. The proposed expression is included in the PM2K software,[25] based on the WPPM algorithm and tested on a ground powder sample of cuprous oxide.

GENERAL PROCEDURE

According to KK, the average contrast factor of any type of dislocation in untextured polycrystalline materials can be written as

$$\bar{C}_{hkl} = \sum_{i,k}^{3} \sum_{j,l}^{2} \bar{G}_{ijkl} E_{ijkl}, \tag{1}$$

where $\mathbf{G}$ and $\mathbf{E}$ are 6×6 symmetrical matrices, respectively known as geometrical and elastic components of the contrast factor. The $\mathbf{G}$ matrix accounts for the orientation of the diffraction vector $\mathbf{d}^*$ in the slip-system of the dislocation

 ©2007 The American Physical Society

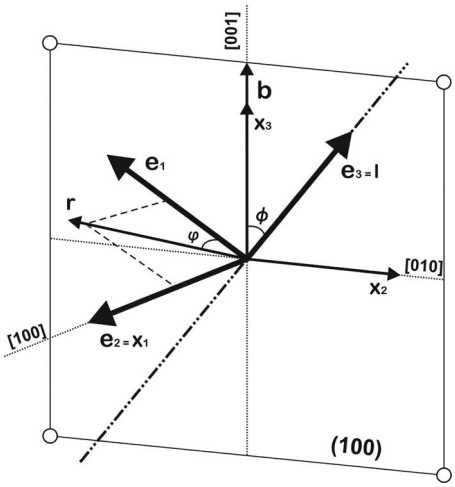

FIG. 1. Infinite straight dislocation on the (100) face of a cubic lattice and the corresponding slip coordinate system $\{\mathbf{e}_k;k=1,2,3\}$. The unit vector $\mathbf{e}_3$ is parallel to the line vector $\mathbf{l}$, $\mathbf{e}_2$ is normal to the slip plane (100), and $\mathbf{e}_1=\mathbf{e}_2\times\mathbf{e}_3$. The quantities $\mathbf{x}_1$, $\mathbf{x}_2$, and $\mathbf{x}_3$ are unit vectors along the crystallographic axes, ϕ is the orientation of the dislocation with respect to its Burgers vector $\mathbf{b}$ (dislocation character), and φ is the integration angle in Eq. (3).

$\{\mathbf{e}_k;k=1,2,3\}$ (see Fig. 1) and it is averaged over the N crystallographically equivalent slip-systems ($\bar{\mathbf{G}}$). The $\mathbf{E}$ matrix takes into account the elastic properties of the material and the displacement field of the dislocation $\mathbf{u}$. Matrix elements can be calculated as

$$G_{ijkl}=(\mathbf{d}^*\cdot\mathbf{e}_i)\,(\mathbf{d}^*\cdot\mathbf{e}_j)\,(\mathbf{d}^*\cdot\mathbf{e}_k)\,(\mathbf{d}^*\cdot\mathbf{e}_l)\,,\quad i,k=1,2,3,\quad j,l=1,2, \tag{2}$$

$$E_{ijkl}=\frac{1}{\pi}\int_0^{2\pi}\beta_{ij}\beta_{kl}d\varphi,\quad i,k=1,2,3,\quad j,l=1,2, \tag{3}$$

$$\beta_{ij}(x_1,x_2)=\frac{2\pi\sqrt{x_1^2+x_2^2}}{b}\frac{\partial u_i(x_1,x_2)}{\partial x_j},\quad i=1,2,3,\quad j=1,2, \tag{4}$$

where $\beta_{ij}(x_1,x_2)$ is proportional to the deformation tensor, u_i is the component of $\mathbf{u}$ referred to $\{\mathbf{e}_k;k=1,2,3\}$, and b is the modulus of the Burgers vector $\boldsymbol{b}$. The coordinates x_1 and x_2 are defined in Fig. 1.

As can be seen from the above equations, first steps in the calculation of $\bar{C}_{hkl}$ are the identification of the equivalent slip-systems and the evaluation of the displacement field of the dislocation. While the analytical evaluation of the $\{\mathbf{e}_k;k=1,2,3\}$ vectors is trivial (once dislocation parameters and crystal metric are known), the determination of analytical expressions for $\mathbf{u}$ in anisotropic materials is not a simple task. Several solutions have been proposed in the literature,[26–29] but actual calculation of $\bar{C}_{hkl}$ was so far based on the Lekhnitskii method, as described in the book of Teodosiu.[30] In the present paper, the Stroh formalism is employed, as it provides the general solution more conveniently in terms of eigenvalues and eigenvectors of a linear eigenvalue problem in the elastic constant representation. As such, the Stroh formalism allows us to obtain, at least for the case of interest in this work, a simple and elegant solution in closed analytical form, thus avoiding the need to introduce Leknitskii's reduced compliance tensor.

It is not the goal of this paper to provide a full discussion of this formalism: a detailed exposition of Stroh's solutions and many examples are given, e.g., by Ting.[31] Here, the essentials of the method useful for the calculation of the contrast factor are briefly illustrated.

According to the Stroh formalism,[27,28,31] the displacement field can be calculated as

$$\mathbf{u}(x_1,x_2)=2\,\mathrm{Re}[\mathbf{A}\cdot\boldsymbol{f}(x_1,x_2)], \tag{5}$$

where Re[] denotes the real part operator, $\mathbf{A}$ is a matrix whose columns are the eigenvectors $\mathbf{A}_\alpha$ with components $\{A_{m\alpha};m=1,2,3\}$, and $\boldsymbol{f}(x_1,x_2)$ is a vector whose elements are the values of a complex potential function $f_\alpha(x_1,x_2)$. In particular, for each eigenvalue p_α,

$$f_\alpha(x_1,x_2)=-\frac{1}{4\pi i}\left(\frac{\mathbf{L}_\alpha\cdot\mathbf{b}}{\mathbf{A}_\alpha\cdot\mathbf{L}_\alpha}\right)\ln(x_1+p_\alpha x_2). \tag{6}$$

The eigenvectors $\mathbf{A}_\alpha$ and the eigenvalues p_α are linked by the following eigenrelation;

$$\{\mathbf{Q}+p_\alpha(\mathbf{R}+\mathbf{R}^t)+p_\alpha^2\mathbf{T}\}\mathbf{A}_\alpha=0, \tag{7}$$

where the t superscript denotes the transpose, and $\mathbf{Q}$, $\mathbf{R}$, and $\mathbf{T}$ are 3×3 matrices related to the single crystal stiffness tensor $\{c_{ijmn};i,j,m,n=1,2,3\}$ by

$$Q_{im}=c_{i1m1},\quad R_{im}=c_{i1m2},\quad T_{im}=c_{i2m2}. \tag{8}$$

Once the eigenvectors $\mathbf{A}_\alpha$ are known, the vectors $\mathbf{L}_\alpha$ in Eq. (6) are determined as

$$\mathbf{L}_\alpha=(\mathbf{R}^t+p_\alpha\mathbf{T})\mathbf{A}_\alpha. \tag{9}$$

Equation (7) has a nontrivial solution if and only if

$$\det[\mathbf{Q}+p_\alpha(\mathbf{R}+\mathbf{R}^t)+p_\alpha^2\mathbf{T}]=0. \tag{10}$$

This yields a sextic equation for p, whose solution is the central problem of the anisotropic elastic theory of linear defects. Equation (10) is equivalent to that obtained by using the Lekhnitskii method.[32] For physically realistic material properties (positive definite strain energy), Eq. (10) has three pairs of complex conjugate roots (eigenvalues), those with positive imaginary part being denoted as p_1, p_2, and p_3. Their three associated eigenvectors $\mathbf{A}_1$, $\mathbf{A}_2$, and $\mathbf{A}_3$ can be obtained from Eq. (7).

Once the eigenvalue problem is solved, the dislocation displacement field can be evaluated by using Eq. (5). The elastic components E_{ijkl} are then calculated by inserting Eq. (5) into Eq. (4) and the result into Eq. (3).

DETERMINING THE ANALYTIC SOLUTION

Eigenvalue problem for ⟨001⟩{001} dislocations

Let us consider an infinite straight dislocation lying on the {100} face of an anisotropic cubic crystal having an arbitrary

orientation ϕ with respect to the Burgers vector $\boldsymbol{b}$ (Fig. 1). We build an orthonormal reference system (slip-system) $\{\mathbf{e}_k;k=1,2,3\}$, so that the vector $\mathbf{e}_3$ is parallel to the dislocation line $\boldsymbol{l}$, thus freeing $\mathbf{u}$ from the dependence on x_3.

In Fig. 1, it is evident that the slip-system vectors $\{\mathbf{e}_k;k=1,2,3\}$ and the unit vectors $\{\mathbf{x}_k;k=1,2,3\}$ are related by

$$\begin{bmatrix} \boldsymbol{x}_1 \\ \boldsymbol{x}_2 \\ \boldsymbol{x}_3 \end{bmatrix} = \mathbf{P} \begin{bmatrix} \mathbf{e}_1 \\ \mathbf{e}_2 \\ \mathbf{e}_3 \end{bmatrix}, \quad \mathbf{P} = \begin{bmatrix} 0 & 1 & 0 \\ -\cos\phi & 0 & \sin\phi \\ \sin\phi & 0 & \cos\phi \end{bmatrix}. \tag{11}$$

To apply the Stroh formalism, it is necessary first to transform the elastic constants defined in the basis vectors $\{\mathbf{x}_k;k=1,2,3\}$ into the slip coordinate system $(c_{ijmn} \rightarrow c'_{ijmn})$:[33]

$$c'_{ijmn} = c_{12}\delta_{ij}\delta_{mn} + c_{44}(\delta_{im}\delta_{jn} + \delta_{in}\delta_{jm}) + H\sum_{r=1}^{3} P_{ri}P_{rj}P_{rm}P_{rn}, \tag{12}$$

where δ_{ij} is Kronecker delta, $H=c_{11}-c_{12}-2c_{44}$, and P_{ri} $(r,i=1,2,3)$ are the elements of the matrix $\mathbf{P}$.

Substitution of Eq. (11) into Eq. (12) yields

$$\begin{aligned} c'_{ijmn} = & \left\{ c_{11} - \frac{H}{2}\sin^2(2\phi)\bar{\delta}_{12} \right\} \delta_{ij}\delta_{mn}\delta_{im} \\ & + \left\{ c_{44} + \frac{H}{2}\sin^2(2\phi)\delta_{i1}\delta_{j3} \right\} \delta_{im}\delta_{jn}\bar{\delta}_{ij} \\ & + \left\{ c_{12} + \frac{H}{2}\sin^2(2\phi)(\delta_{i1}\delta_{m3} + \delta_{i3}\delta_{m1}) \right\} \delta_{ij}\delta_{mn}\bar{\delta}_{im} \\ & + \frac{H}{4}\sin(4\phi)(\delta_{j3}\delta_{n3}\delta_{|i-m|,2} - \delta_{i1}\delta_{m1}\delta_{|j-n|,2}), \end{aligned} \tag{13}$$

where $\bar{\delta}_{ij}=1-\delta_{ij}$. By using Eqs. (13) and (8), the three matrices $\mathbf{Q}$, $\mathbf{R}$, and $\mathbf{T}$ can now easily be evaluated in terms of the elastic constants c_{ijmn}:

$$\mathbf{Q} = \begin{bmatrix} c_{11} - \frac{1}{2}H\sin^2(2\phi) & 0 & -\frac{1}{4}H\sin(4\phi) \\ 0 & c_{44} & 0 \\ -\frac{1}{4}H\sin(4\phi) & 0 & c_{44} + \frac{1}{2}H\sin^2(2\phi) \end{bmatrix}, \tag{14}$$

$$\mathbf{R} = \begin{bmatrix} 0 & c_{12} & 0 \\ c_{44} & 0 & 0 \\ 0 & 0 & 0 \end{bmatrix}, \quad \mathbf{T} = \begin{bmatrix} c_{44} & 0 & 0 \\ 0 & c_{11} & 0 \\ 0 & 0 & c_{44} \end{bmatrix}. \tag{15}$$

Therefore, in the studied ⟨001⟩{001} slip-system, the sextic equation (10) for a straight dislocation of character ϕ takes the form

$$p^6 + [1+\eta_0]p^4 + [1+\eta_0+\kappa_1(\phi)]p^2 + [1+\kappa_2(\phi)] = 0. \tag{16}$$

The roots with positive imaginary part have the form

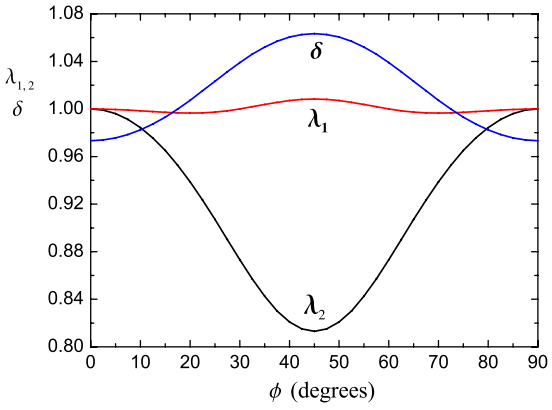

FIG. 2. (Color online) Variation with the dislocation character ϕ of moduli λ_1 and λ_2 and phase δ of the p roots.

$$p_1 = -\lambda_1 e^{-i\delta}, \quad p_2 = \lambda_1 e^{i\delta}, \quad p_3 = \lambda_2 i. \tag{17}$$

Analytic expressions for η_0, $\kappa_1(\phi)$, $\kappa_2(\phi)$, λ_1, λ_2, and δ are given in the Appendix.

Figure 2 illustrates the dependence of magnitude $\lambda_{1,2}$ and phase δ of the p roots with ϕ. In the limit cases of screw $(\phi=0)$ and edge $(\phi=\pi/2)$ orientations, $\kappa_1(\phi)=\kappa_2(\phi)=0$ and thus Eq. (16) admits simple solutions of the form

$$p_1 = \frac{1}{2}(-\sqrt{2-\eta_0} + i\sqrt{2+\eta_0}),$$

$$p_2 = \frac{1}{2}(\sqrt{2-\eta_0} + i\sqrt{2+\eta_0}),$$

$$p_3 = i. \tag{18}$$

The associated eigenvectors $\{\mathbf{A}_\alpha;\alpha=1,2,3\}$ are determined by inserting Eq. (18) into Eq. (7) and solving a $[3\times3]$ homogeneous equation system for each eigenvalue, respectively.

$$\mathbf{A}_\alpha = \varsigma_1 \begin{bmatrix} -\dfrac{p_\alpha^2 c_{11} + c_{44}}{(p_\alpha^2 c_{11} - c_{12})c_{44}} \\ \dfrac{p_\alpha(c_{12}+c_{44})}{(p_\alpha^2 c_{11} - c_{12})c_{44}} \\ 0 \end{bmatrix}, \quad \mathbf{A}_3 = \varsigma_1 \begin{bmatrix} 0 \\ 0 \\ i/c_{44} \end{bmatrix}. \tag{19}$$

Hence, the $\{\mathbf{L}_\alpha;\alpha=1,2,3\}$ vectors in Eq. (9) have the form

$$\boldsymbol{L}_1 = \varsigma_2 \begin{bmatrix} -p_1 \\ 1 \\ 0 \end{bmatrix}, \quad \boldsymbol{L}_2 = \varsigma_2 \begin{bmatrix} -p_2 \\ 1 \\ 0 \end{bmatrix}, \quad \boldsymbol{L}_3 = \varsigma_2 \begin{bmatrix} 0 \\ 0 \\ 1 \end{bmatrix}. \tag{20}$$

Actual values of the complex constants ς_1 and ς_2 do not enter calculations [cf. Eq. (6)].

Elastic component of the contrast factor

The evaluation of the elastic component of the contrast factor E_{ijkl} is straightforward once the solutions of the eigen-

value problem are known. If a is the unit cell parameter, the Burgers vector in the dislocation slip-system can be represented as $[0,0,a]$ and $[a,0,0]$ for screw and edge orientations, respectively. Thus, by inserting Eqs. (19) and (20) into Eq. (6) and the result into Eq. (5), the complex potential $f_\alpha(x_1,x_2)$ and the displacement field components $\{\mathbf{u}_k;k=1,2,3\}$ become

$$f_\alpha(x_1,x_2) = \begin{cases} [ia\ln(x_1+p_3x_2)/4\pi A_{33}]\delta_{\alpha 3}, & \phi=0 \\ [ia\ln(x_1+p_\alpha x_2)/4\pi A_{1\alpha}(\Lambda_\alpha+1)]\bar{\delta}_{\alpha 3}, & \phi=\pi/2, \end{cases} \tag{21}$$

$$u_k(x_1,x_2) = \begin{cases} [ia\ln(x_1+p_3x_2)/2\pi]\delta_{k3}, & \phi=0 \\ \sum_{\alpha=1}^{2}[ia\ln(x_1+p_\alpha x_2)/4\pi A_{1\alpha}(\Lambda_\alpha+1)]\bar{\delta}_{k3}, & \phi=\pi/2, \end{cases} \tag{22}$$

where $\Lambda_\alpha=(c_{12}+c_{44})/(p_\alpha^2 c_{11}+c_{44})$ and $\alpha=1,2,3$.

By using the above formulas, an analytical solution can be found for the deformation tensor and thus for the integrals in Eq. (3). In particular, for the edge dislocation, the nonzero elements of the elastic matrix E_{ijkl} are

$$E_{1111}=\frac{4\kappa_1}{\sqrt{2+\eta_0}}\left\{1+\frac{(1-\gamma_1)(2+\eta_0)}{4(1+\gamma_0)}\right\},$$

$$E_{2211}=\kappa_1\sqrt{2+\eta_0}\left\{1+\frac{2(\eta_0-2\gamma_1)}{(2+\eta_0)(1+\gamma_0)}\right\},$$

$$E_{1221}=-\kappa_1\sqrt{2+\eta_0}\left\{1+\frac{2(2-\eta_0\gamma_1)}{(2+\eta_0)(1+\gamma_0)}\right\},$$

$$E_{1212}=\frac{4\kappa_1}{\sqrt{2+\eta_0}}\left\{1+\frac{(2+\eta_0)[\gamma_1(1-\eta_0)+1]}{4(1+\gamma_0)}\right\},$$

$$E_{2222}=\frac{4\kappa_1}{\sqrt{2+\eta_0}}\left\{1+\frac{(2+\eta_0)(\eta_0-\gamma_1-1)}{4(1+\gamma_0)}\right\},$$

$$E_{2121}=E_{1111},$$

$$\kappa_1=\frac{(1+\gamma_0)}{(2+\gamma_0)^2-\gamma_1^2},\quad \gamma_0=\frac{c_{12}}{c_{44}},\quad \gamma_1=\frac{c_{11}}{c_{44}}, \tag{23}$$

whereas the only nonzero terms are $E_{3131}=E_{3232}=1$ in the screw case.

Analytical expression for $\bar{C}_{hkl}$

Unlike E_{ijkl}, the geometrical component G_{ijkl} can be easily calculated in cubic lattices. The terms $\mathbf{d}^*\cdot\mathbf{e}_i$ in Eq. (2) can be evaluated in the $\{\mathbf{e}_k;k=1,2,3\}$ system as

$$\mathbf{d}^*\cdot\mathbf{e}_i=\frac{hu_i+kv_i+lw_i}{(h^2+k^2+l^2)^{1/2}}, \tag{24}$$

where h,k,l are the Miller indices and (u_i,v_i,w_i) the coordinates of $\mathbf{e}_i$ in $\{\mathbf{x}_k;k=1,2,3\}$ (i.e., the ith column of the $\mathbf{P}$ matrix). Therefore, the elements of the geometrical matrix are

$$G_{ijkl}=\frac{(hu_i+kv_i+lw_i)(hu_j+kv_j+lw_j)}{h^2+k^2+l^2} \times\frac{(hu_k+kv_k+lw_k)(hu_l+kv_l+lw_l)}{h^2+k^2+l^2}. \tag{25}$$

For the case under study, the total number of crystallographically equivalent slip-systems $\{\mathbf{e}_k;k=1,2,3\}$ is $N=6$ (i.e., 3 slip planes $\times 2$ slip directions per plane). By averaging the values of Eq. (25) for each equivalent slip-system for both edge and screw orientations, and taking into account Eqs. (23) and (1), the average dislocation contrast factor can be written as

$$\bar{C}_{hkl}=A+B\frac{h^2k^2+k^2l^2+l^2h^2}{(h^2+k^2+l^2)^2}, \tag{26}$$

where

$$A=\begin{cases}0, & \phi=0\\ (2-\eta_1)/3\sqrt{2+\eta_0}, & \phi=\pi/2,\end{cases} \tag{27}$$

$$B=\begin{cases}2/3, & \phi=0\\ (\eta_2-2)/3\sqrt{2+\eta_0}, & \phi=\pi/2,\end{cases} \tag{28}$$

in which

$$\eta_1=\frac{(1-2\nu)[1+A_z\nu(1-2\nu)]}{(1-\nu)^2[1+A_z(1-2\nu)]}, \tag{29}$$

$$\eta_2=\frac{(4\nu^3-4\nu^2+3\nu-1)A_z^2-2\nu A_z+2(1-\nu)}{A_z(1-\nu)^2[1+A_z(1-2\nu)]}. \tag{30}$$

Equation (26) gives the average dislocation contrast factor in anisotropic cubic materials as a fourth order crystallographic invariant of the Miller indices. The coefficients A and B in Eq. (26) are given by Eqs. (27) and (28) as analytic functions of two dimensionless physical parameters: Zener ratio A_z and Poisson ratio ν, directly related to the elastic constants. This allows us to evaluate A and B, and therefore $\bar{C}_{hkl}$, in a straightforward way, avoiding the need for numerical methods or approximate parametric expressions.

Figures 3(a) and 3(b) show, respectively, the dependence of A and B on the anisotropic factor A_z for several values of ν.

APPLICATION TO BALL MILLED Cu_2O

Materials and methods

To validate the procedures proposed in this work, we selected a commercial anhydrous Cu_2O powder (Sigma-

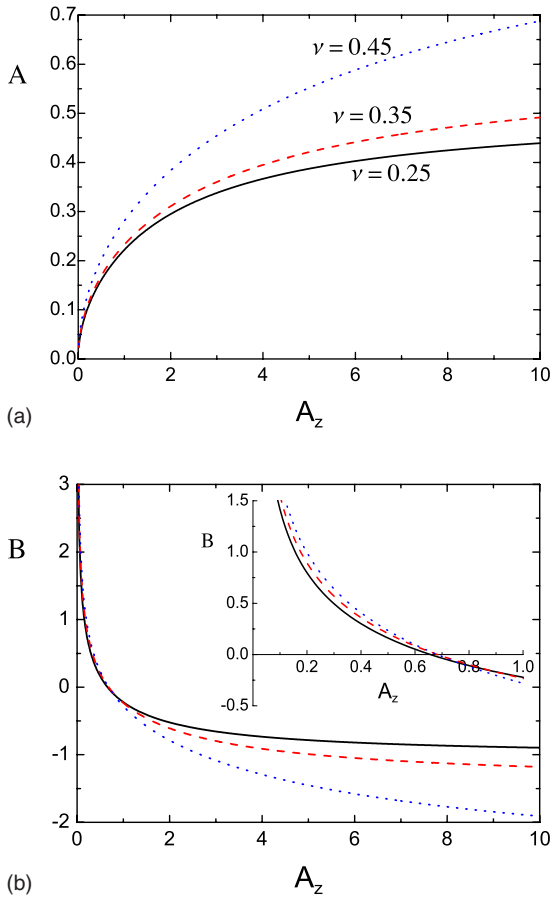

FIG. 3. (Color online) Variation of the parameters (a) A and (b) B for edge dislocations as a function of anisotropy factor A_z and Poisson ratio: ν=0.25 (line), ν=0.35 (dash), and ν=0.45 (dot).

Aldrich, 99.99+% purity) that was ground for 5 min in a high-energy shutter mill (Fritsch P9). To avoid overheating, with possible annealing effects, grinding was made in 30 stages, each consisting of 10 s grinding followed by 120 s cooling at room temperature (25 °C). Details on the milling process can be found elsewhere.[34]

The x-ray diffraction measurement was performed on a Rigaku PMG-VH diffractometer operated at 40 kV and 30 mA. The machine is equipped with a secondary crystal analyzer and an optical setup consisting of 1° divergence slit, 2° Soller slit, 1° antiscatter slit, 2° secondary Soller slits, and a 0.15 mm receiving slit, providing a narrow and symmetrical instrumental profile for approximately $2\theta > 20°$. In order to get high quality data, the pattern was collected in step scan mode from 18° to 154°, with a step size of 0.1° and a fixed acquisition time of 150 s per point.

Whole powder pattern modeling

The pattern was modeled by the PM2K software,[25] based on the WPPM approach. Details on the procedure can be found, e.g., in the cited references.[6–9]

WPPM allows the analysis of powder diffraction data in terms of physical models of the microstructure and lattice defects, without using arbitrarily chosen analytical profiles. Since the diffraction profile (I_{hkl}) is a convolution of profile components due to the different line broadening sources,[6–9,35] the WPPM algorithm is conveniently based on the Fourier transform (FT) of each profile component:

$$I_{hkl}(s) = k(s) \int T^{IP}(L) A^S(L) A^D_{hkl}(L) e^{2\pi i L s} dL, \qquad (31)$$

where $s = d^* - d^*_B$ is the reciprocal space variable ($\mathbf{d}^*_B$ is $\mathbf{d}^*$ in Bragg condition) that can also be written as $s = 2 \sin\theta/\lambda - 2 \sin\theta_B/\lambda$, with θ_B and λ as Bragg angle and wavelength, respectively. $k(s)$ is a known function of s, including Lorentz-polarization factor, absorption terms, and square modulus of the structure factor. T^{IP} is the FT of the instrumental profile (IP), which is generally known [previously determined using a line profile standard[8] such as the NIST SRM 660a LaB_6 (Ref. 36)], whereas A^S and A^D_{hkl} are FTs of the profile components due to crystalline domain size and dislocations, respectively. The Fourier variable L is the distance along $\mathbf{d}^*$ between couples of unit cells. Additional FTs can be added to Eq. (31) if necessary,[6–9] but in the present case, besides the IP, it is enough to consider domain size effects and dislocations only.

Concerning size effects, we assume domains as spherical, with diameters dispersed according to a generic discrete distribution $g_h(D)$, for which one can write[37]

$$A^S(L) = \frac{\int_L^\infty D^3 A^S_s(L,D) g_h(D) dD}{\int_0^\infty D^3 g_h(D) dD}, \qquad (32)$$

where

$$A^S_s(L,D) = 1 - \frac{3}{2}\frac{L}{D} + \frac{1}{2}\left(\frac{L}{D}\right)^3 \qquad (33)$$

is the FT for a spherical crystalline domain of diameter D.

Dislocation effects are considered according to the Krivoglaz-Wilkens theory:[3–5]

$$A^D_{hkl}(L) = \exp\left[-\frac{1}{2}\pi b^2 \bar{C}_{hkl} \rho d^{*2}_B L^2 f^*(L/R_e) \right], \qquad (34)$$

where ρ is the average dislocation density, R_e is the effective outer cut-off radius, and f^* is a known function[5] of L/R_e. In the present case, we implemented Eqs. (26)–(28) to express $\bar{C}_{hkl}$ and introduced the effective screw and/or edge dislocation character f_E through

$$\bar{C}_{hkl} = f_E \bar{C}^E_{hkl} + (1 - f_E) \bar{C}^S_{hkl}, \qquad (35)$$

where the superscripts E and S refer to edge and screw dislocations, respectively. The average contrast factor is in any case a function of A_z, ν, and hkl, but in this way, we can refine the dislocation character based on the specific degree of line broadening anisotropy in the studied powder.

In conclusion, the microstructural parameters refined by WPPM are ρ, R_e, f_E, and the size distribution histogram. Additional parameters, not directly influencing the microstructure and the line broadening, are the unit cell parameter

a, the displacement of the specimen from the goniometer axis (a typical error in powder diffraction measurements), the coefficients of a Chebyshev polynomial background, and peak intensities. An advantage of the WPPM with respect to most traditional LPA procedures is the possibility to account for multiple phases with no changes in the algorithm. This feature is especially useful for the present case of study.

RESULTS AND DISCUSSION

Cuprous oxide (cuprite, Cu_2O) is a technologically important material, with potential applications in sensors, magnetic storage, solar cells, and many other microelectronic devices.[38,39] From the mechanical point of view, Cu_2O is rather peculiar because its shear modulus ($G=10.3$ GPa) is comparatively low with respect to other oxides and most metals. Such a low G, which means a low dislocation specific energy ($\propto Gb^2$), is a prerequisite to incorporate a high density of dislocations during plastic deformation.[24]

The commercial powder contained a small fraction of metallic Cu particles, showing weak but sharp diffraction peaks. Moreover, several weak reflections, that appeared after the grinding, can be attributed to the higher oxidation state oxide, CuO (tenorite). Modeling thus included three phases (with corresponding crystallographic space group): Cu_2O (cuprite, Pn-3m), Cu (fcc copper, Fm-3m), and CuO (tenorite, Cc).

Owing to the low (monoclinic) symmetry, tenorite displays a large number of weak and overlapping peaks. To improve the reliability of the modeling, CuO intensities were fixed to the value calculated from the known crystal structure [FIZ Card No. 69094 (Ref. 40)] using a pattern simulation software (JPOWD).[46] In this way, only one parameter (a scale factor) was refined for the tenorite peak intensities. Moreover, as the slip-system of tenorite is not known, following a recently proposed procedure,[19] the strain broadening anisotropy in this minor phase was accounted for by modeling the coefficients of the fourth order invariant form for the Laue group of tenorite ($2/m$). Strain broadening in copper was modeled assuming dislocations being present on the $\frac{1}{2}\langle 1-10\rangle\{111\}$ primary slip-system for fcc metals. Cuprite elastic constants, to be used in Eqs. (26)–(28), are $c_{11}=121$, $c_{12}=105$, and $c_{44}=12.1$ GPa.[41]

Figure 4 shows the WPPM result for the ball milled cuprite powder. As shown by the featureless residual, the quality of the cuprite modeling is fairly good, despite the interfering presence of Cu and CuO. The domain size distribution for cuprite is shown in Fig. 5. The main fraction is centered around 6.2 nm, even though there is a minor fraction of about 15 nm. The mean value for the other two minor phases is just approximate, owing to the weak diffraction signal, and gives ~90(30) nm for copper and ~11(3) nm for tenorite.

As to the dislocation density, the value for cuprite is quite high, $\rho=2.8(5)\times 10^{16}$ m^{-2}, with an effective outer cut-off radius $R_e=9(3)$ nm. The effective dislocation character is $f_E=0.85(3)$, which points out a predominance of edge dislocations. The extent of line broadening anisotropy can be appreciated in Fig. 6, where the average contrast factor given by Eq. (35) for the refined f_E value is shown. Calculated limiting cases for edge and screw dislocations are also reported.

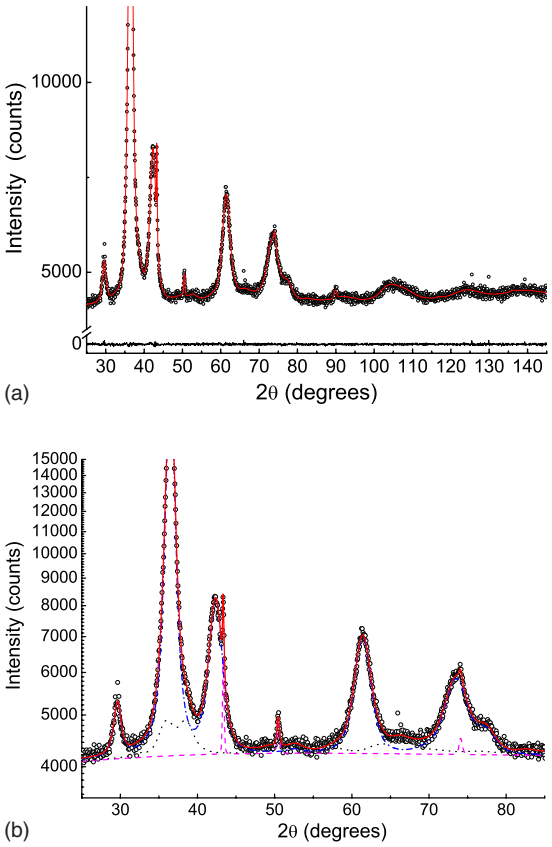

FIG. 4. (Color online) (a) WPPM results for the ball milled cuprite powder: data (dot), modeling result (line), and residual (difference between data and model, line below). In (b), the result is reported in logarithmic scale to highlight the contributions of the present phases: Cu_2O (dash-dot), Cu (dash), and CuO (dot). [Quality indices (Ref. 45): $R_{wp}=1.527\%$, $R_{expt}=1.400\%$, GoF=1.091; data points=2401, degrees of freedom=2281.]

Finally, Wilkens' parameter, $R_e\sqrt{\rho}=1.5$, is well within the validity limits of the theory[5,11] and suggests a strong dislocation interaction.

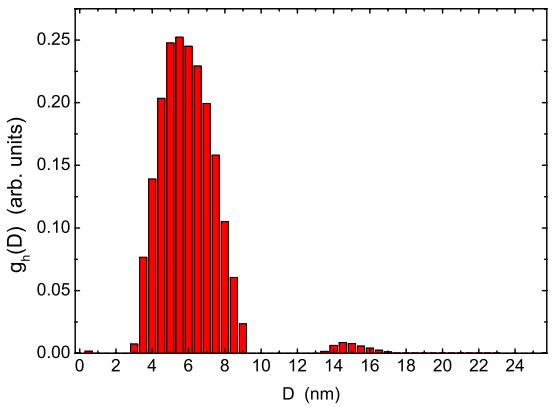

FIG. 5. (Color online) Spherical domain diameter distribution obtained by WPPM for the Cu_2O phase.

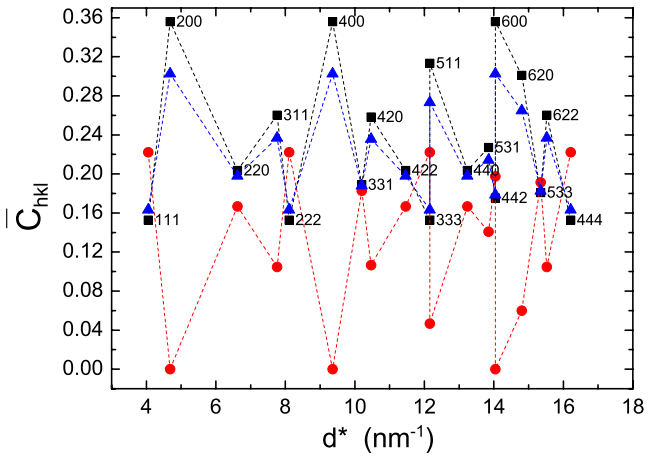

FIG. 6. (Color online) Average contrast factor as function of the diffraction vector for several reflections of Cu_2O (Miller indices are shown near each data point): calculated values for edge (square) and screw (circle) dislocations in the ⟨100⟩{001} slip-system and experimentally refined values (triangle).

The refined dislocation density in copper is about $1.6(12)\times10^{15}$ m^{-2}. Even though this value, for the low intensity of the copper signal, is affected by a large error, it appears that grinding had little effect on the few metal particles present in the cuprite commercial powder. This would also be confirmed by the relatively large domain size for copper and is in agreement with the fact that, commonly, to produce measurable effects in metal powders much longer grinding times are needed.[42] As to tenorite, no dislocation density is available because the slip-system is not known, and in any case, the phase content would be too small to give a reliable result. It is significant, however, that the domain size of tenorite is significantly larger than that of cuprite, an observation at least compatible with several literature results suggesting that a smaller domain size is a stabilization mechanism of cuprite with respect to the thermodynamically stable tenorite.[24,43,44]

The dislocation density in cuprite is about half of the value found in wear debris of a copper-beryllium alloy.[24] Also in that case, a CuO minority fraction was found, and its presence was related to the domain size stabilization effect of Cu_2O. In the same study, transmission electron microscopy showed the presence of some edge dislocations, that were also the prevailing type according to WPPM.

CONCLUSIONS

The dislocation contrast factor is the main parameter to represent the anisotropic nature of the dislocation strain field and its effects on diffraction phenomena. So far, this important parameter could only be calculated numerically, with lengthy procedures to be carried out each time for a specific material and slip system. In this work, we demonstrated that by exploiting the symmetry conditions of specific slip-systems and crystal structures, it is possible to calculate an analytical expression for the average dislocation contrast factor.

In particular, this was shown for the ⟨001⟩{100} slip-system in cubic materials, for which $\bar{C}_{hkl}$ can be written in a closed analytical form, as a function of *hkl*, the anisotropy factor A_z, and the Poisson ratio ν.

The validity of this approach was tested on a Cu_2O powder plastically deformed by high-energy milling. The analytical $\bar{C}_{hkl}$ expression was included in a general whole powder pattern modeling algorithm and used to determine the dislocation density and other microstructural parameters in the ground powder.

Besides the quality and detail of information obtainable from this approach, it is important to underline that the same procedure can easily be used for structures isomorphic to Cu_2O, just by using the corresponding elastic constants. Analytical expressions for other slip-systems are to be published in the next future.

ACKNOWLEDGMENTS

J.M.-G. is particularly grateful for financial support to the University of Trento-University of Havana joint collaboration agreement and to Sincrotrone Trieste S.C.p.A (ELETTRA synchrotron) for hospitality during the time this research activity was carried out.

APPENDIX: ANALYTIC SOLUTIONS OF THE SEXTIC EQUATION

The analytic expressions for the elastic parameters which appear in sextic equation (16) are

$$\kappa_1(\phi) = \sin^2(2\phi)(A_z^{-1} - 1)\left(\eta_0 - A_z^{-1} - \frac{c_{44}}{c_{11}}\right),$$

$$\kappa_2(\phi) = \sin^2(2\phi)\left(\frac{\eta_0 - 2}{4}\right),$$

$$\eta_0 = \frac{2(1-\nu A_z)}{A_z(1-\nu)},$$

$$A_z = \frac{2c_{44}}{c_{11}-c_{12}},$$

$$\nu = \frac{c_{12}}{c_{11}+c_{12}}. \tag{A1}$$

It should be noticed that in the isotropic limit, $A_z=1$, $\eta_0=2$, and $\kappa_{1,2}(\phi)=0$; thus, Eq. (16) is reduced to the well known characteristic equation for isotropic materials: $(p^2+1)^3=0$.

The constants λ_1, λ_2, and δ in Eq. (17) are given by

$$\lambda_1 = \sqrt{\frac{[1+\kappa_2(\phi)]^{1/2}}{\lambda_2}},$$

$$\lambda_2 = \sqrt{S + 2\sqrt{R}\sinh(x)}, \quad x = \frac{1}{3}\operatorname{arcsinh}\left(\frac{Q}{2\sqrt{R^3}}\right),$$

$$\delta = \frac{1}{2}\arccos\left(\frac{\lambda_2^2 - 3S}{2\lambda_1^2}\right), \tag{A2}$$

where

$$S = \frac{\eta_0 + 1}{3},$$

$$R = S(1-S) + \frac{1}{3}\kappa_1(\phi),$$

$$Q = 1 - S(S^2 + 3R) + \kappa_2(\phi). \tag{A3}$$

*paolo.scardi@unitn.it

[1] A. C. McLaren, *Transmission Electron Microscopy of Minerals and Rocks* (Cambridge University Press, Cambridge UK, 1991).
[2] A. J. C. Wilson, Acta Crystallogr. **5**, 318 (1952).
[3] M. A. Krivoglaz and K. P. Ryaboshapka, Fiz. Met. Metalloved. **15**, 18 (1963).
[4] M. A. Krivoglaz, *Theory of X-ray and Thermal Neutron Scattering by Real Crystals* (Plenum, New York, 1969).
[5] M. Wilkens, *Fundamental Aspects of Dislocation Theory*, Natl. Bur. Stand. (U.S.) Spec. Publ. No. 317, edited by J. A. Simmons, R. de Wit, R. Bullough, (U.S. GPO, Washington, D.C., 1970), Vol. II, pp. 1195–1221.
[6] P. Scardi and M. Leoni, Acta Crystallogr., Sect. A: Found. Crystallogr. **57**, 604 (2001).
[7] P. Scardi and M. Leoni, Acta Crystallogr., Sect. A: Found. Crystallogr. **A58**, 190 (2002).
[8] P. Scardi and M. Leoni, in *Diffraction Analysis of the Microstructure of Materials*, edited by E. J. Mittemeijer and P. Scardi (Springer-Verlag, Berlin, 2004), pp. 51–91.
[9] P. Scardi and M. Leoni, Acta Mater. **53**, 5229 (2005).
[10] N. Armstrong, M. Leoni, and P. Scardi, Z. Kristallogr. Suppl. **23**, 81 (2006).
[11] M. A. Krivoglaz, *X-ray and Neutron Diffraction in Nonideal Crystals* (Springer-Verlag, Berlin, 1996).
[12] M. Wilkens, Phys. Status Solidi A **104**, K1 (1987).
[13] P. Klimanek and R. Kužel, J. Appl. Crystallogr. **21**, 59 (1988).
[14] R. Kužel and P. Klimanek, J. Appl. Crystallogr. **21**, 363 (1988).
[15] P. Klimanek and R. Kužel, J. Appl. Crystallogr. **22**, 299 (1989).
[16] T. Ungár and G. Tichy, Phys. Status Solidi A **171**, 425 (1999).
[17] T. Ungár, I. Dragomir, Á. Révész, and A. Borbély, J. Appl. Crystallogr. **32**, 992 (1999).
[18] I. C. Dragomir and T. Ungár, J. Appl. Crystallogr. **35**, 556 (2002).
[19] M. Leoni, J. Martinez-Garcia, and P. Scardi, J. Appl. Crystallogr. **40**, 719 (2007).
[20] A. K. Head, J. Elast. **9**, 9 (1979).
[21] N. Armstrong and P. Lynch, in *Diffraction Analysis of the Microstructure of Materials*, edited by E. J. Mittemeijer and P. Scardi (Springer-Verlag, Berlin, 2004), pp. 249–286.
[22] J. W. Steeds, *Introduction to Anisotropic Elasticity Theory of Dislocations* (Oxford University Press, London, 1973).
[23] G. Vagnard and J. Washburn, J. Am. Ceram. Soc. **51**, 88 (1968).
[24] P. Scardi, M. Leoni, G. Straffelini, and G. De Giudici, Acta Mater. **55**, 2531 (2007).
[25] M. Leoni, T. Confente, and P. Scardi, Z. Kristallogr. Suppl. **23**, 249 (2006).
[26] J. D. Eshelby, Acta Metall. **1**, 251 (1953).
[27] A. N. Stroh, Philos. Mag. **7**, 625 (1958).
[28] A. N. Stroh, J. Math. Phys. **41**, 77 (1963).
[29] S. G. Leknitskii, *Theory of Elasticity of an Anisotropic Elastic Body* (Holden-Day, San Francisco, 1963).
[30] C. Teodosiou, *Elastic Models of Crystal Defects* (Springer-Verlag, Berlin, 1978).
[31] T. C. T. Ting, *Anisotropic Elasticity: Theory and Applications* (Oxford University Press, New York, 1996).
[32] D. M. Barnett and H. O. K. Kirchner, Philos. Mag. A **76**, 231 (1997).
[33] T. Y. Thomas, Proc. Natl. Acad. Sci. U.S.A. **55**, 235 (1966).
[34] D. Dodoo-Arhin, J. Martinez-Garcia, M. Leoni, and P. Scardi (unpublished).
[35] H. P. Klug and L. E. Alexander, *X-ray Diffraction Procedures for Polycrystalline and Amorphous Materials* (Wiley, New York, 1974).
[36] J. P. Cline, R. D. Deslattes, J.-L. Staudenmann, E. G. Kessler, L. T. Hudson, A. Hennins, and R. W. Cheary, NIST Certificate (SRM 660a) Line Position and Line Shape Standard for Power Diffraction, Gaithersburg USA, NIST Standard Reference Materials Program, NIST, USA (2000).
[37] M. Leoni and P. Scardi, J. Appl. Crystallogr. **37**, 629 (2004).
[38] J. Zhang, J. Liu, Q. Peng, X. Wang, and Y. Li, Chem. Mater. **18**, 867 (2006).
[39] P. J. Sebastian, J. Quintana, F. Avila, and X. Mathew, Surf. Eng. **16**, 47 (2000).
[40] http://www.fiz-karlsruhe.de/
[41] A. G. Every and A. K. McCurdy, in *Crystal and Solid State Physics*, edited by D. F. Nelson, Landolt-Börnstein, New Series, group III, Vol. 29 (Springer, Berlin, 1992), p. 68.
[42] C. C. Koch, Nanostruct. Mater. **2**, 109 (1993).
[43] V. R. Palkar, P. Ayyub, S. Chattopadhyay, and M. Multani, Phys. Rev. B **53**, 2167 (1996).
[44] P. Scardi and M. Leoni, Mater. Sci. Eng., A **393**, 396 (2005).
[45] L. B. McCusker, R. B. Von Dreele, D. E. Cox, D. Louër, and P. Scardi, J. Appl. Crystallogr. **32**, 36 (1999).
[46] JPOWD, Version 5.2, MDI.